ARL-MR-1084 ● SEP 2023

Robotic Photovoltaic Cell Testing

by Angel Ayala, Stefan Gutierrez, and David R Baker

NOTICES

Disclaimers

The findings in this report are not to be construed as an official Department of the Army position unless so designated by other authorized documents.

Citation of manufacturer's or trade names does not constitute an official endorsement or approval of the use thereof.

Destroy this report when it is no longer needed. Do not return it to the originator.

ARL-MR-1084 ● SEP 2023

Robotic Photovoltaic Cell Testing

Angel Ayala and Stefan Gutierrez
National Security Innovation Network (NSIN) X-Force Fellow

David R Baker
DEVCOM Army Research Laboratory

REPORT DOCUMENTATION PAGE

1. REPORT DATE	2. REPORT TYPE	3. DATES COVERED	
		START DATE	END DATE
September 2023	Memorandum Report	5 June 2023	11 August 2023

4. TITLE AND SUBTITLE
Robotic Photovoltaic Cell Testing

5a. CONTRACT NUMBER	5b. GRANT NUMBER	5c. PROGRAM ELEMENT NUMBER
5d. PROJECT NUMBER	**5e. TASK NUMBER**	**5f. WORK UNIT NUMBER**

6. AUTHOR(S)
Angel Ayala, Stefan Gutierrez, and David R Baker

7. PERFORMING ORGANIZATION NAME(S) AND ADDRESS(ES)	8. PERFORMING ORGANIZATION REPORT NUMBER
DEVCOM Army Research Laboratory ATTN: FCDD-RLA-GC Adelphi, MD 20783-1138	ARL-MR-1084

9. SPONSORING/MONITORING AGENCY NAME(S) AND ADDRESS(ES)	10. SPONSOR/MONITOR'S ACRONYM(S)	11. SPONSOR/MONITOR'S REPORT NUMBER(S)
National Security Innovation Network: 2121 Crystal Drive, Suite 500, Arlington, VA 22202 National Institute for Standards and Technology: 100 Bureau Drive, Gaithersburg, MD 20899		

12. DISTRIBUTION/AVAILABILITY STATEMENT
DISTRIBUTION STATEMENT A. Approved for public release: distribution unlimited.

13. SUPPLEMENTARY NOTES
ORCID ID: David Baker, 0000-0002-9930-5183

14. ABSTRACT
During the 2023 X-Force Fellowship Program, DEVCOM Army Research Laboratory researchers collaborated with the National Institute of Standards and Technology to control robotic-mounted photovoltaic (PV) cells on a six-axis robot. The objective was to further understand the efficiency of PV cells under different lighting conditions as well as the response to angular manipulations and positioning about a light source. This research would allow the Department of Defense to create and design better PV panels to supply more energy power to deployed Soldiers.

15. SUBJECT TERMS
X-Force, photovoltaics, diffuse light, solar energy, robotics, Energy Sciences

16. SECURITY CLASSIFICATION OF:			17. LIMITATION OF ABSTRACT	18. NUMBER OF PAGES
a. REPORT	b. ABSTRACT	C. THIS PAGE		
UNCLASSIFIED	UNCLASSIFIED	UNCLASSIFIED	UU	21

19a. NAME OF RESPONSIBLE PERSON	19b. PHONE NUMBER *(Include area code)*
David R Baker	(301) 394-2249

STANDARD FORM 298 (REV. 5/2020)
Prescribed by ANSI Std. Z39.18

Contents

List of Figures

List of Tables

1. Introduction

During the 2023 X-Force Fellowship Program, US Army Combat Capabilities Development Command Army Research Laboratory (ARL) researchers collaborated with the National Institute of Standards and Technology (NIST) to control robotic-mounted photovoltaic (PV) cells on a six-axis robot. The objective was to further understand the efficiency of PV cells under different lighting conditions and the response to angular manipulations and positioning about a light source. This research would allow the Department of Defense to create and design enhanced PV panels to supply more energy power to deployed Soldiers. For example, when out on a 3-day mission, Soldiers carry over 20 lb of batteries to power their devices, but with better PV equipment, that space could be utilized for more crucial supplies, such as medicine. The findings from this study will allow researchers to create impactful tactical power solutions.

1.1 Background

The National Renewable Energy Laboratory is the leader in research for PV cell data. However, their research is focused on developing efficient capture of direct solar irradiance on flat PV devices. PV cells are semiconductors that convert sunlight into electricity. Angular variations are crucial to understanding light and energy effects on PV cells because environmental factors in everyday life are not always flat. Understanding how different cell orientations will affect energy output is particularly beneficial in military applications for deployed Soldiers, especially in diffused light conditions. A Soldier's light environment is constantly changing in terms of angle surfaces, shading, or elevation (distance from the sun). The Universal Robot series 5e (UR5e), used during this study, is a six-axis robot that moves based on tool face coordinates or joint positions. This flexibility of movement and position is significant because it allows data to be collected and analyzed in various positions and orientations. Engineers can thus simulate virtually any environmental condition that a Soldier or civilian would encounter.

1.2 Hypothesis

The objective of this project was to program and use a six-axis robot to accurately measure energy output from an external light source onto a PV cell. It was crucial to gather data on diffused light to accurately mimic real-world conditions. Our initial projections and hypotheses for this project were two-fold. We hypothesized that we would be using text-based coding, such as Python, and controlling the universal robot using a single moving algorithm. We also hypothesized that the PV

cell would gather less current and energy whenever the cell was not in a facing degree orientation in respect to the external light source. In relation, the PV cell would gather less energy in the diffused condition due to having less light directed into the cell compared to non-diffused conditions.

2. Experiment

The X-force fellows performed the experimentation at NIST, creating a program that controls the robot's movements and provides the necessary functionalities to conduct testing and data acquisition. The robot is controlled by a user-friendly user interface using the LabView development environment that offers the necessary controls and output data necessary for an easy-to-use program. Currently, the robot can be manipulated to scan through X-Y-Z Cartesian coordinates in space and control the tool face's tool center point. The input controls allow for a start and end point in meters for the position, while the tool face controls allow for start and end positions in degrees. The user can specify the "step size" or the distance between waypoints. The program does the necessary calculations and provides an array via the front panel showing the waypoints used during the sweep. The tool face has the reference cell attached via an adaptor plate, allowing the user to control the angular position of the reference cell around the light source.

The program can confirm that the robot is at a specified position through a built-in function to ensure that the reference cell location is within parameters of an allowable standard deviation. Currently, the program checks that the position of the reference cell about the light source is within 2.01E-5 cm from the user-specified positions created by the waypoint algorithm. The reference cell on the tool face also performs the same position check algorithm while undergoing angular changes where the deviation tolerance is within 0.0035 of a degree, allowing us to ensure that the data acquisition process supplies precise data for further analysis. The process of verifying that the deviation is less than the allowable tolerances is done three times to ensure the reference cell's position is correct. If the deviation check fails, the program flags the value on the text output to notify that the position was greater than the allowed deviation.

3. Results

Figures 1–10 are intensity maps that illustrate the current and energy output from a reference cell in different orientations and various positions in space. This data consists of an uncollimated light source with no diffusion of light. We ran a sweep parameter, and the robot coordinated itself to each position. In those positions, the robot communicated with a Keithley multimeter and waited in each position for enough time to allow the multimeter to calculate and gather the current emitted from the PV cell. For the linear portions (Figs. 1–7) we input sweep values to make the robot position itself from complete darkness (out of range) to the middle range, allowing us to compare intensity and current. For the rotation portions (Figs. 8–10), we kept the PV cell in one plane and rotated it in the x, y, z, allowing us to compare intensities among all orientations in that single plane and point.

	A	B	C	D	E	F	G	H
1	X (m)	Y (m)	Z (m)	Rx (deg)	RY (deg)	RZ (deg)	Current	Verificartion
2	-0.25	0.4	0.22	0.00177	2.21976	2.22153	-1.4E-05	1
3	-0.15	0.4	0.22	0.00177	2.21976	2.22153	-1.9E-05	1
4	-0.05	0.4	0.22	0.00177	2.21976	2.22153	-1.9E-05	1
5	0.05	0.4	0.22	0.00177	2.21976	2.22153	-2E-05	1
6	0.15	0.4	0.22	0.00177	2.21976	2.22153	-2.2E-05	1
7	0.25	0.4	0.22	0.00177	2.21976	2.22153	-6.4E-07	1
8	0.25	0.4	0.32	0.00177	2.21976	2.22153	-1.4E-05	1
9	0.15	0.4	0.32	0.00177	2.21976	2.22153	-2E-05	1
10	0.05	0.4	0.32	0.00177	2.21976	2.22153	-2E-05	1
11	-0.05	0.4	0.32	0.00177	2.21976	2.22153	-2.1E-05	1
12	-0.15	0.4	0.32	0.00177	2.21976	2.22153	-1.9E-05	1
13	-0.25	0.4	0.32	0.00177	2.21976	2.22153	-1.9E-05	1
14	-0.25	0.4	0.42	0.00177	2.21976	2.22153	-1.9E-05	1
15	-0.15	0.4	0.42	0.00177	2.21976	2.22153	-2E-05	1
16	-0.05	0.4	0.42	0.00177	2.21976	2.22153	-2.1E-05	1
17	0.05	0.4	0.42	0.00177	2.21976	2.22153	-2.1E-05	1
18	0.15	0.4	0.42	0.00177	2.21976	2.22153	-1.9E-05	1
19	0.25	0.4	0.42	0.00177	2.21976	2.22153	-1.7E-05	1
20	0.25	0.4	0.52	0.00177	2.21976	2.22153	-5.6E-06	1
21	0.15	0.4	0.52	0.00177	2.21976	2.22153	-2E-05	1
22	0.05	0.4	0.52	0.00177	2.21976	2.22153	-1.9E-05	1
23	-0.05	0.4	0.52	0.00177	2.21976	2.22153	-1.9E-05	1
24	-0.15	0.4	0.52	0.00177	2.21976	2.22153	-1.7E-05	1
25	-0.25	0.4	0.52	0.00177	2.21976	2.22153	-1.8E-05	1
26	-0.25	0.4	0.62	0.00177	2.21976	2.22153	-1.7E-06	1
27	-0.15	0.4	0.62	0.00177	2.21976	2.22153	-1.6E-05	1
28	-0.05	0.4	0.62	0.00177	2.21976	2.22153	-1.8E-05	1
29	0.05	0.4	0.62	0.00177	2.21976	2.22153	-1.9E-05	1
30	0.15	0.4	0.62	0.00177	2.21976	2.22153	-9.9E-06	1
31	0.25	0.4	0.62	0.00177	2.21976	2.22153	-3.9E-07	1
32	0.25	0.4	0.72	0.00177	2.21976	2.22153	-2.6E-07	1
33	0.15	0.4	0.72	0.00177	2.21976	2.22153	-4.2E-07	1
34	0.05	0.4	0.72	0.00177	2.21976	2.22153	-5.2E-07	1
35	-0.05	0.4	0.72	0.00177	2.21976	2.22153	-6.8E-07	1
36	-0.15	0.4	0.72	0.00177	2.21976	2.22153	-4.6E-07	1
37	-0.25	0.4	0.72	0.00177	2.21976	2.22153	-3.7E-07	1

Fig. 1 Raw data, 40 cm from base in the y direction

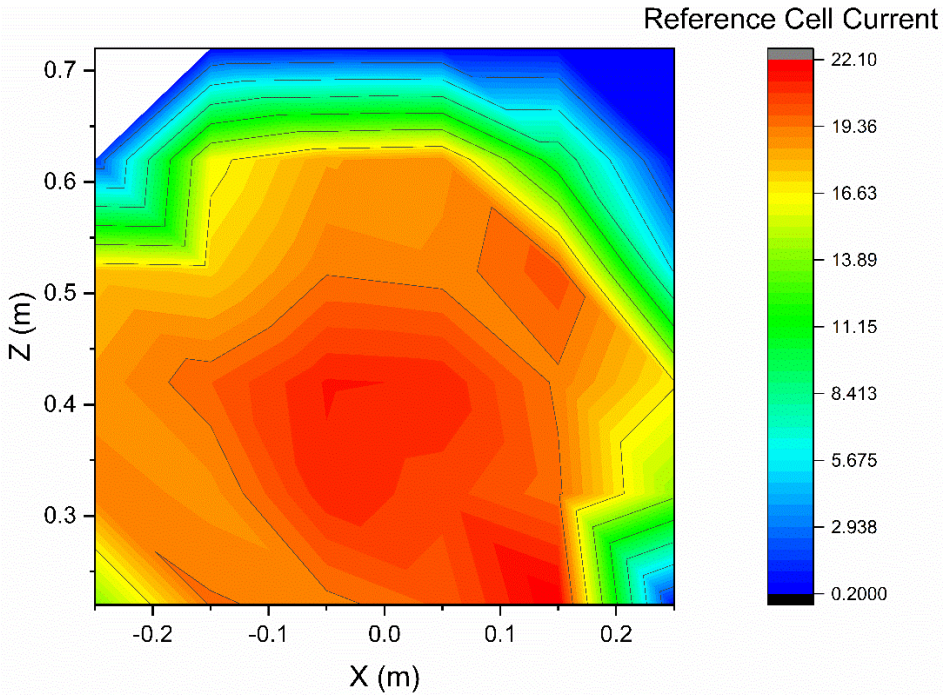

Fig. 2 Intensity map, 40 cm from base in the y direction

	A	B	C	D	E	F	G	H	I
1	X (m)	Y (m)	Z (m)	Rx (deg)	RY (deg)	RZ (deg)	Current	Verificartion	
2	-0.25	0.5	0.22	0.00177	2.21976	2.22153	-4.9E-06	1	
3	-0.15	0.5	0.22	0.00177	2.21976	2.22153	-2.5E-05	1	
4	-0.05	0.5	0.22	0.00177	2.21976	2.22153	-2.3E-05	1	
5	0.05	0.5	0.22	0.00177	2.21976	2.22153	-2.4E-05	1	
6	0.15	0.5	0.22	0.00177	2.21976	2.22153	-2.4E-05	1	
7	0.25	0.5	0.22	0.00177	2.21976	2.22153	-4E-07	1	
8	0.25	0.5	0.32	0.00177	2.21976	2.22153	-3.5E-06	1	
9	0.15	0.5	0.32	0.00177	2.21976	2.22153	-2.4E-05	1	
10	0.05	0.5	0.32	0.00177	2.21976	2.22153	-2.4E-05	1	
11	-0.05	0.5	0.32	0.00177	2.21976	2.22153	-2.5E-05	1	
12	-0.15	0.5	0.32	0.00177	2.21976	2.22153	-2.2E-05	1	
13	-0.25	0.5	0.32	0.00177	2.21976	2.22153	-2.2E-05	1	
14	-0.25	0.5	0.42	0.00177	2.21976	2.22153	-2.2E-05	1	
15	-0.15	0.5	0.42	0.00177	2.21976	2.22153	-2.3E-05	1	
16	-0.05	0.5	0.42	0.00177	2.21976	2.22153	-2.5E-05	1	
17	0.05	0.5	0.42	0.00177	2.21976	2.22153	-2.5E-05	1	
18	0.15	0.5	0.42	0.00177	2.21976	2.22153	-2.3E-05	1	
19	0.25	0.5	0.42	0.00177	2.21976	2.22153	-8E-06	1	
20	0.25	0.5	0.52	0.00177	2.21976	2.22153	-7.5E-07	1	
21	0.15	0.5	0.52	0.00177	2.21976	2.22153	-2.4E-05	1	
22	0.05	0.5	0.52	0.00177	2.21976	2.22153	-2.2E-05	1	
23	-0.05	0.5	0.52	0.00177	2.21976	2.22153	-2.2E-05	1	
24	-0.15	0.5	0.52	0.00177	2.21976	2.22153	-2.1E-05	1	
25	-0.25	0.5	0.52	0.00177	2.21976	2.22153	-1.6E-05	1	
26	-0.25	0.5	0.62	0.00177	2.21976	2.22153	-6.7E-07	1	
27	-0.15	0.5	0.62	0.00177	2.21976	2.22153	-1.4E-05	1	
28	-0.05	0.5	0.62	0.00177	2.21976	2.22153	-2.1E-05	1	
29	0.05	0.5	0.62	0.00177	2.21976	2.22153	-2E-05	1	
30	0.15	0.5	0.62	0.00177	2.21976	2.22153	-3.6E-06	1	
31	0.25	0.5	0.62	0.00177	2.21976	2.22153	-3.4E-07	1	
32	0.25	0.5	0.72	0.00177	2.21976	2.22153	-1.9E-07	1	
33	0.15	0.5	0.72	0.00177	2.21976	2.22153	-3.5E-07	1	
34	0.05	0.5	0.72	0.00177	2.21976	2.22153	-5.4E-07	1	
35	-0.05	0.5	0.72	0.00177	2.21976	2.22153	-5.2E-07	1	
36	-0.15	0.5	0.72	0.00177	2.21976	2.22153	-5.7E-07	1	
37	-0.25	0.5	0.72	0.00177	2.21976	2.22153	(Ctrl)	1	

Fig. 3 Raw data, 50 cm from base in the y direction

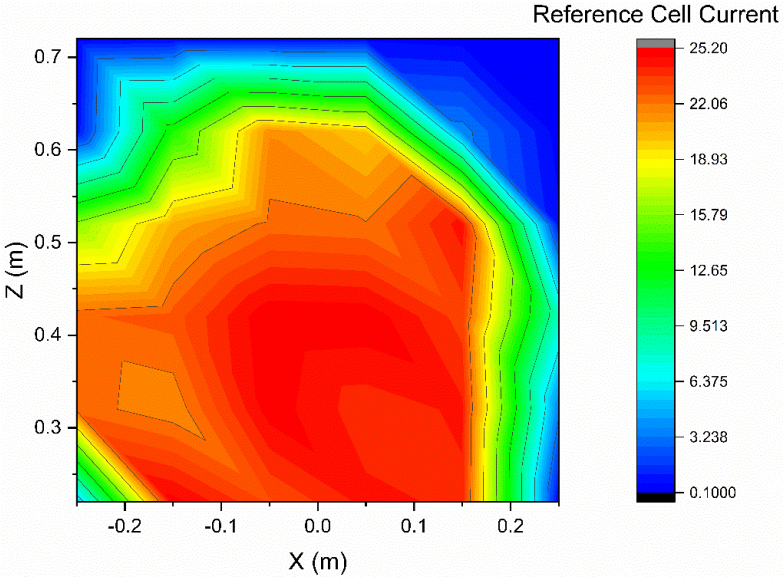

Fig. 4 Intensity map, 50 cm from base in the y direction

	A	B	C	D	E	F	G	H
1	X (m)	Y (m)	Z (m)	Rx (deg)	RY (deg)	RZ (deg)	Current	Verificartion
2	-0.25	0.6	0.22	0.00177	2.21976	2.22153	-7.9E-07	1
3	-0.15	0.6	0.22	0.00177	2.21976	2.22153	-2.9E-05	1
4	-0.05	0.6	0.22	0.00177	2.21976	2.22153	-2.9E-05	1
5	0.05	0.6	0.22	0.00177	2.21976	2.22153	-3.2E-05	1
6	0.15	0.6	0.22	0.00177	2.21976	2.22153	-9.7E-06	1
7	0.25	0.6	0.22	0.00177	2.21976	2.22153	-4.6E-07	1
8	0.25	0.6	0.32	0.00177	2.21976	2.22153	-5.5E-07	1
9	0.15	0.6	0.32	0.00177	2.21976	2.22153	-3.1E-05	1
10	0.05	0.6	0.32	0.00177	2.21976	2.22153	-2.8E-05	1
11	-0.05	0.6	0.32	0.00177	2.21976	2.22153	-3E-05	1
12	-0.15	0.6	0.32	0.00177	2.21976	2.22153	-2.5E-05	1
13	-0.25	0.6	0.32	0.00177	2.21976	2.22153	-2.1E-05	1
14	-0.25	0.6	0.42	0.00177	2.21976	2.22153	-2.5E-05	1
15	-0.15	0.6	0.42	0.00177	2.21976	2.22153	-2.7E-05	1
16	-0.05	0.6	0.42	0.00177	2.21976	2.22153	-3E-05	1
17	0.05	0.6	0.42	0.00177	2.21976	2.22153	-3E-05	1
18	0.15	0.6	0.42	0.00177	2.21976	2.22153	-2.9E-05	1
19	0.25	0.6	0.42	0.00177	2.21976	2.22153	-7.6E-07	1
20	0.25	0.6	0.52	0.00177	2.21976	2.22153	-4.7E-07	1
21	0.15	0.6	0.52	0.00177	2.21976	2.22153	-2.7E-05	0
22	0.05	0.6	0.52	0.00177	2.21976	2.22153	-2.6E-05	1
23	-0.05	0.6	0.52	0.00177	2.21976	2.22153	-2.6E-05	1
24	-0.15	0.6	0.52	0.00177	2.21976	2.22153	-2.5E-05	1
25	-0.25	0.6	0.52	0.00177	2.21976	2.22153	-8.2E-06	1
26	-0.25	0.6	0.62	0.00177	2.21976	2.22153	-7.1E-07	1
27	-0.15	0.6	0.62	0.00177	2.21976	2.22153	-6.6E-06	0
28	-0.05	0.6	0.62	0.00177	2.21976	2.22153	-2.1E-05	1
29	0.05	0.6	0.62	0.00177	2.21976	2.22153	-1.6E-05	1
30	0.15	0.6	0.62	0.00177	2.21976	2.22153	-7.3E-07	1
31	0.25	0.6	0.62	0.00177	2.21976	2.22153	-3.7E-07	1
32	0.25	0.6	0.72	0.00177	2.21976	2.22153	-1.3E-07	1
33	0.15	0.6	0.72	0.00177	2.21976	2.22153	-3.4E-07	1
34	0.05	0.6	0.72	0.00177	2.21976	2.22153	-5.2E-07	1
35	-0.05	0.6	0.72	0.00177	2.21976	2.22153	-6.4E-07	1
36	-0.15	0.6	0.72	0.00177	2.21976	2.22153	-4.1E-07	1
37	-0.25	0.6	0.72	0.00177	2.21976	2.22153	-2.8E-07	1
38								

Fig. 5 Raw data, 60 cm from base in the y direction

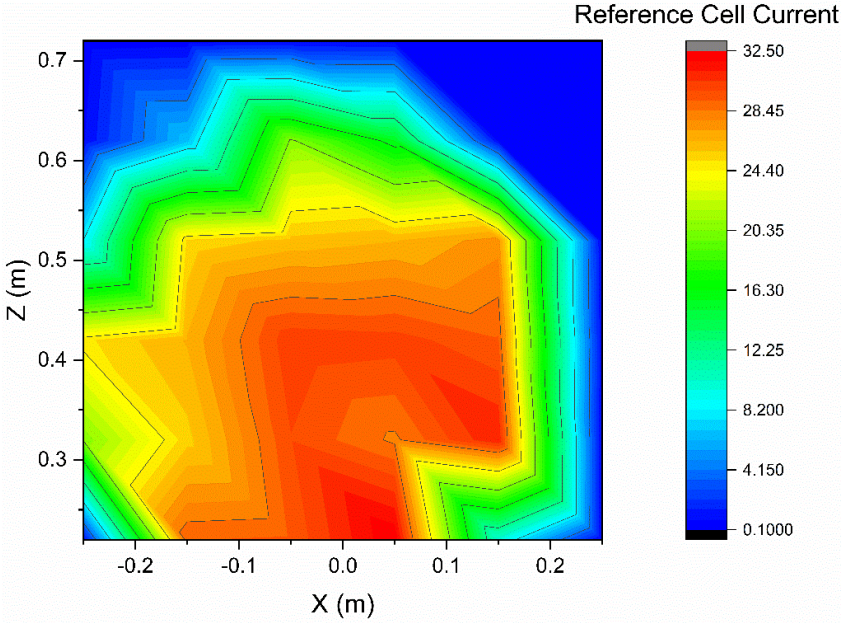

Fig. 6 Intensity map, 60 cm from base in the y direction

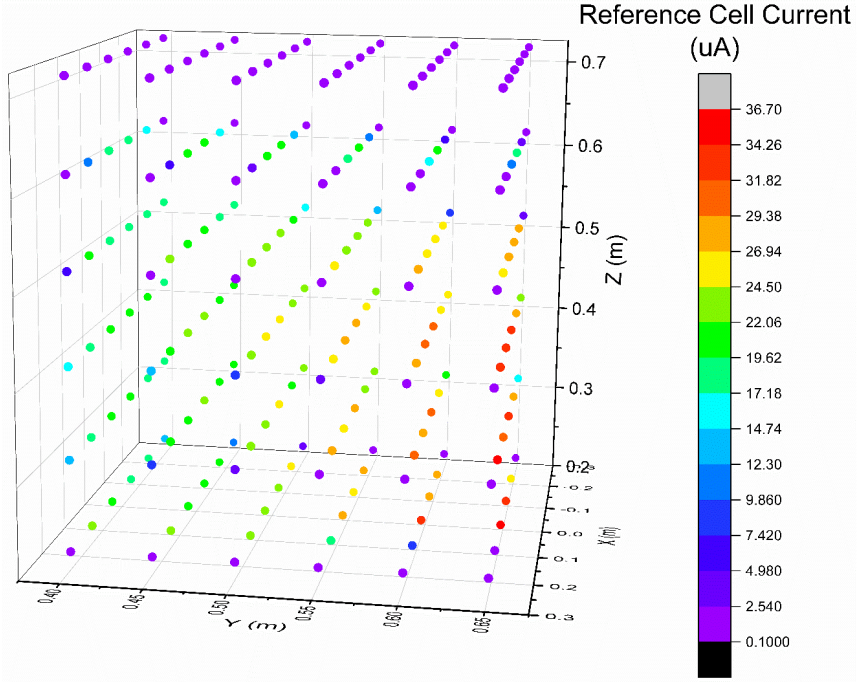

Fig. 7 Three-plane intensity view (XYZ)

	A	B	C	D	E	F	G	H
1	X (m)	Y (m)	Z (m)	Rx (deg)	RY (deg)	RZ (deg)	Current	verficatior
2	-0.03	0.5	0.42	0.3794	0.92091	2.20888	-0.00001	1
3	-0.03	0.5	0.42	0.45832	1.11245	2.13682	-1.3E-05	1
4	-0.03	0.5	0.42	0.5356	1.30005	2.05076	-1.5E-05	1
5	-0.03	0.5	0.42	0.61531	1.49353	1.94439	-1.6E-05	1
6	-0.03	0.5	0.42	0.68824	1.67053	1.82954	-1.7E-05	1
7	-0.03	0.5	0.42	0.76255	1.85091	1.69276	-1.7E-05	1
8	-0.03	0.5	0.42	0.82961	2.01369	1.54931	-1.6E-05	1
9	-0.03	0.5	0.42	0.89685	2.17691	1.38245	-1.5E-05	1
10	-0.03	0.5	0.42	0.95637	2.32136	1.21088	-1.3E-05	0
11	-0.03	0.5	0.42	1.01465	2.46283	1.01465	-0.00001	0
12	-0.03	0.5	0.42	0.31095	0.98496	2.36252	-1.3E-05	1
13	-0.03	0.5	0.42	0.37521	1.18851	2.28291	-1.5E-05	1
14	-0.03	0.5	0.42	0.4379	1.38708	2.18805	-1.8E-05	1
15	-0.03	0.5	0.42	0.50224	1.59087	2.07111	-1.9E-05	1
16	-0.03	0.5	0.42	0.56074	1.7762	1.94527	-0.00002	1
17	-0.03	0.5	0.42	0.61995	1.96374	1.79594	-0.00002	1
18	-0.03	0.5	0.42	0.67293	2.13154	1.63999	-1.9E-05	1
19	-0.03	0.5	0.42	0.72552	2.29813	1.45943	-1.7E-05	1
20	-0.03	0.5	0.42	0.7715	2.44379	1.27474	-1.5E-05	1
21	-0.03	0.5	0.42	0.81588	2.58436	1.06472	-1.2E-05	1
22	-0.03	0.5	0.42	0.23062	1.05206	2.52346	-1.5E-05	1
23	-0.03	0.5	0.42	0.27791	1.26776	2.43514	-1.8E-05	1
24	-0.03	0.5	0.42	0.32381	1.47719	2.33018	-0.00002	1
25	-0.03	0.5	0.42	0.37065	1.69083	2.20125	-2.2E-05	1
26	-0.03	0.5	0.42	0.41293	1.88373	2.06303	-2.2E-05	1
27	-0.03	0.5	0.42	0.45535	2.07725	1.89976	-2.2E-05	1
28	-0.03	0.5	0.42	0.49293	2.24866	1.7301	-2.1E-05	1
29	-0.03	0.5	0.42	0.52978	2.41675	1.53477	-0.00002	1
30	-0.03	0.5	0.42	0.56153	2.56159	1.33619	-1.7E-05	1
31	-0.03	0.5	0.42	0.59162	2.69886	1.11189	-1.4E-05	1
32	-0.03	0.5	0.42	0.14662	1.11461	2.67349	-1.6E-05	1
33	-0.03	0.5	0.42	0.17643	1.34117	2.57614	-1.9E-05	1
34	-0.03	0.5	0.42	0.20521	1.56	2.46081	-2.2E-05	1
35	-0.03	0.5	0.42	0.23439	1.78178	2.31965	-2.3E-05	1
36	-0.03	0.5	0.42	0.26053	1.98047	2.16898	-2.4E-05	1
37	-0.03	0.5	0.42	0.28651	2.17797	1.99186	-2.4E-05	1
38								

Fig. 8 Rotation raw data

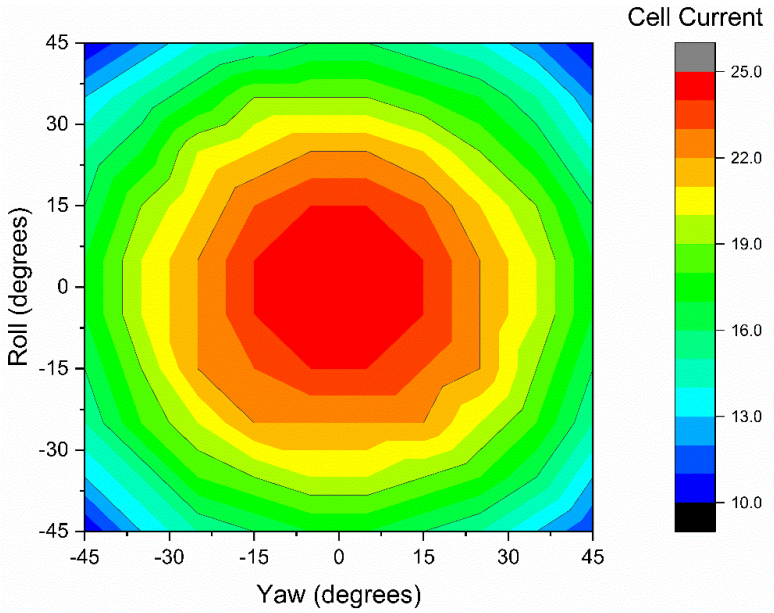

Fig. 9 Rotation intensity map

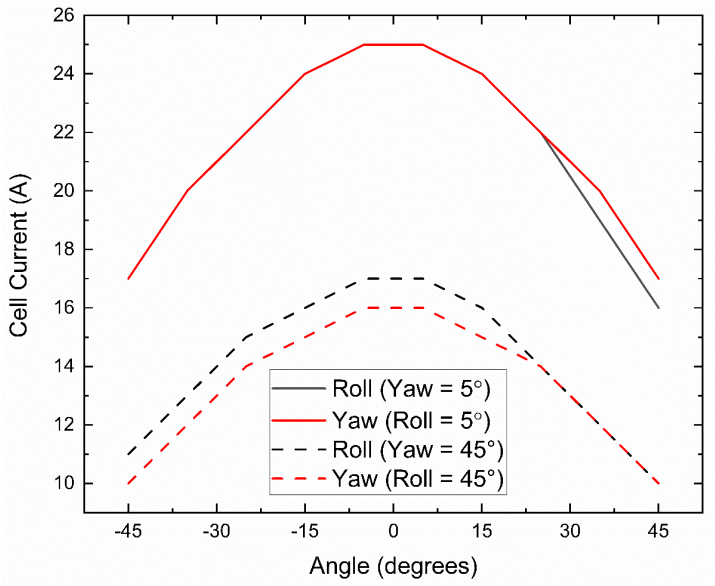

Fig. 10 Rotation wave

4. Discussion

As illustrated in the previous section, the current is highest when the PV center is directly in line with the center of the light course. As the PV cell increases its distance from the cell in linear space, the current output decreases. Similarly, if the angle between the PV and light source center points increases, the current decreases. In addition, as the PV cell rotates, the current decreases, which is

particularly evident in Fig. 10. This change is due to the intensity of the light—as the cell tilts, some portions of the cell will be farther way than other portions, therefore the whole cell will not receive the same amount of light.

For safety and verification purposes, a program was implemented to allow the user and coder to analyze and determine whether the robot was positioned in the right orientation and plane. The user inputs the values they wish to sweep, and when the program is finished, it outputs the robot positions and compares the two values, showing whether each position matched or not. For this verification data shown in Table 1, we acquired data from four sweep runs with various X-Y-Z coordinates as well as various roll-pitch-yaw (rotation) coordinates. This allowed us to calculate the best deviation tolerance. We implemented a tolerance check allowing a 2-standard-deviation tolerance; if the user input and the robot output did not fall within that tolerance, the output would display a "0" as shown in Figs. 1, 3, 5, and 8, and the researcher can decide to exclude that unreliable data point in their analysis.

Table 1 Verification data

Runs	1	2	3	4	Total
X error (m)	1.2581E-05	1.4919E-05	1.1210E-05	1.0403E-05	1.25806E-05
X STDV (m)	1.0885E-05	1.1996E-05	9.7608E-06	9.14199E-06	1.08853E-05
Y error (m)	7.25806E-06	5.16129E-06	1.02419E-05	8.79032E-06	7.25806E-06
Y STDV (m)	6.9069E-06	5.77123E-06	9.83305E-06	8.51519E-06	6.9069E-06
Z error (m)	1.23387E-05	1.26613E-05	1.59677E-05	1.45161E-05	1.23387E-05
Z STDV (m)	1.0753E-05	1.13416E-05	1.36697E-05	1.25818E-05	1.07529E-05
RX error (deg)	0.002868	0.002612	0.026508	0.002297	0.002868
RX STDV (deg)	0.001889	0.002082	0.002928	0.001721	0.001889
RY error (deg)	0.002277	0.001875	0.001971	0.001977	0.002277
RY STDV (deg)	0.00159	0.001521	0.001691	0.001608	0.00159
RZ error (deg)	0.002341	0.002202	0.00233	0.002162	0.002341
RZ STDV (deg)	0.00175	0.001558	0.001776	0.00177	0.00175

Combined standard deviations (2 standard deviations for verification)	XYZ: 2.01E-5 m	RPY: 0.0035°

5. Future Directions

Due to time constraints of the fellowship, we have not taken data with diffused light or enough data with uncollimated light. An ideal next step in the research would be continuing the data acquisition with additional sweeps and data points with non-diffused collimated light as a control group. Next would be analyzing different light environments by attaching light-diffusing filters to collimated and uncollimated light sources to simulate different conditions. With those data points, researchers can compare control groups with the diffused group and use that data to analyze the energy output between collimated/uncollimated and diffused/ undiffused sunlight. To aid in the data collection, we recommend using a monochromator to eliminate any unwanted light that would negatively affect the PV readings.

In terms of programming, the following future objectives should be considered:

- Programming the sweep functionality to allow the robot to stay within a diameter of an uncollimated light source in various Y planes as illustrated in Fig. 11. This would allow the user to input sweep coordinates while the PV remains in plane of the external light source, running for hours without the assistance of the user. In addition, this would help with data implementation, as the user would not need to filter out the data points of the PV cell being in complete darkness. In relation, this would cut down robot sweep time so the data can be analyzed faster.

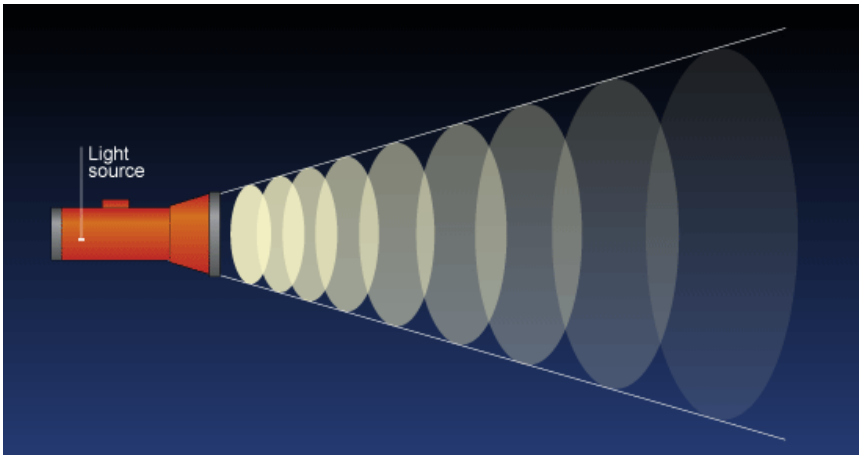

Fig. 11 Uncollimated light source

- Understanding and implementing a user joint interface and the inverse kinematics associated with that interface. Currently, the program is designed to take in tool face coordinates, and the robot moves each joint independently to complete the position movement. However, the joint

movement interface would do the opposite of the tool face interface. The user could input joint positions and the robot would coordinate the tool face in the positions based on the joint locations. This type of movement can be helpful to overcome the UR5e internal joint revolution limitation and safety guards. Each joint on the robot has limitations set, so currently, if the engineer puts in a tool position and the joints are set in the proximity of its revolution limits, then the robot will lock up and throw an error. In relation, if one joint is too close to another joint, the robot will disable itself and also throw an error on the control screen. The ability to move by joints may allow the robot to be fully automated without human interference.

6. Conclusion

Understanding PV cells on a broader scale is crucial to advancing solar energy in civilian and miliary applications. This scale includes various positions, angles, and light conditions, such as diffused light. The UR5e makes this significantly easier and faster. In addition, this process is repeatable with less error. Applying different filters also becomes easier and provides spatial consistency between tested devices. The current data shows that the energy out of the PV is not uniform, and there are hotspots throughout the light source. With this universal robot, we are steps closer to providing Soldiers with more efficient power instruments for batteries and other tactical equipment.

List of Symbols, Abbreviations, and Acronyms

ARL	Army Research Laboratory
DEVCOM	US Army Combat Capabilities Development Command
NIST	National Institute of Standards and Technology
PV	photovoltaic
UR5e	Universal Robot series 5e

1 (PDF)	DEFENSE TECHNICAL INFORMATION CTR DTIC OCA
1 (PDF)	DEVCOM ARL FCDD RLB CI TECH LIB
1 (PDF)	DEVCOM ARL FCDD RLA GC D BAKER
1 (PDF)	TEXAS TECH UNIVERSITY A AYALA
1 (PDF)	NORTHEASTERN UNIVERSITY S GUTIERREZ
2 (PDF)	NIST A SHORE B HAMADANI